



THE UNIVERSITY *of* EDINBURGH

Edinburgh Research Explorer

## Uncertainty Quantification of Geo-Magnetically Induced Currents in UHV Power Grid

**Citation for published version:**

Liu, Q, Xie, Y, Dong, N, Chen, Y, Liu, M & Li, Q 2020, 'Uncertainty Quantification of Geo-Magnetically Induced Currents in UHV Power Grid', *IEEE Transactions on Electromagnetic Compatibility*, vol. 62, no. 1, pp. 258 - 265. <https://doi.org/10.1109/TEMC.2019.2894945>

**Digital Object Identifier (DOI):**

[10.1109/TEMC.2019.2894945](https://doi.org/10.1109/TEMC.2019.2894945)

**Link:**

[Link to publication record in Edinburgh Research Explorer](#)

**Document Version:**

Peer reviewed version

**Published In:**

IEEE Transactions on Electromagnetic Compatibility

**General rights**

Copyright for the publications made accessible via the Edinburgh Research Explorer is retained by the author(s) and / or other copyright owners and it is a condition of accessing these publications that users recognise and abide by the legal requirements associated with these rights.

**Take down policy**

The University of Edinburgh has made every reasonable effort to ensure that Edinburgh Research Explorer content complies with UK legislation. If you believe that the public display of this file breaches copyright please contact [openaccess@ed.ac.uk](mailto:openaccess@ed.ac.uk) providing details, and we will remove access to the work immediately and investigate your claim.



# Uncertainty Quantification of Geo-Magnetically Induced Currents in UHV Power Grid

Qing Liu , Yan-zhao Xie , *Member, IEEE*, Ning Dong, Yu-hao Chen, Min-zhou Liu, and Quan Li 

**Abstract**—Geo-magnetically induced currents (GICs) have attracted more attention since many Ultra-High Voltage (UHV) transmission lines have been built, or are going to be built in the world. However, when calculating GICs based on the classical model, some input parameters, such as the earth conductivity and dc resistances of the grid, are uncertain or very hard to be determined in advance. Taking this into account, the uncertainty quantification (UQ) model of the geo-electric fields and GICs is proposed in this paper. The UQ of the maximums of the geo-electric fields and GICs during storms is carried out based on the polynomial chaos (PC) method. The results of the UHV grid, 1000 kV Sanhua Grid, were presented and compared to the Monte Carlo method. The total Sobol indices are calculated by using the PC expansion coefficients. The sensitivities of geo-electric fields and GICs to the input variables are analyzed based on the total Sobol indices. Results show that the GICs and geo-electric fields can be effectively simulated by the proposed model, which may offer a better understanding of the sensitivities to input uncertain variables and further give a reasonable evaluation of the geomagnetic threat to the grid.

**Index Terms**—Geo-electric fields, Geo-magnetically induced currents (GIC), polynomial chaos (PC), total Sobol indices, uncertainty quantification (UQ).

## I. INTRODUCTION

SOLAR activities, especially coronal mass ejections, solar flares, and energetic particles, are the major factors that affect space weather and trigger geomagnetic disturbances (GMDs). The GMDs can induce low-frequency currents into power networks, known as geo-magnetically induced currents (GICs) [1]–[3]. The GICs may cause half-cycle saturation in

power transformers, produce harmonics, and increase reactive power demand and transformer spot heat. This can lead to serious problems, such as transformer damage, voltage dips, relay disoperation, and system instability [4]–[6]. Although GMDs are more likely to happen in high latitudes, recently the phenomenon caused by GICs are also found in middle and low latitudes [7], [8], such as South Africa, Brazil, and China, which attracts broad attention.

GIC calculation requires the induced geo-electric fields over the earth's surface. The "source" of this geo-electric field (i.e., the magnetosphere-ionosphere currents) can be approximately determined by an infinite line current, surface current, or three-dimensional (3-D) current model. There are a number of methods based on different assumptions and simplifications that can be used to calculate the geo-electric fields and the GICs. A simple way is to apply an equivalent downward-propagating plane wave and assume that the earth is either uniform or layered [9]. A lot of work on geo-electric fields and GICs has been reported with specific parameters [10]–[15].

However, some input parameters are difficult to be precisely quantified, particularly in large scale power systems. For example, the earth conductivity along the depth of several hundred kilometers is an approximation of the actual structure due to the multiplicity on magnetotelluric inversion and noise interference [16]. Since the frequency of geo-electromagnetic variations is far less than that of electric power, the resistances play a dominant role for GIC calculation and the power grid can approximately be equivalent to a dc network [17]. For GIC calculation, the dynamic characteristics of ac voltages and transformer saturation should be taken into consideration. As an engineering approach, nevertheless, to model the network as resistances is more acceptable. The dc resistances of transmission lines and the transformer windings should be regarded as variables due to their changes with temperatures and should be taken into consideration.

The Ultra-High Voltage power grid is the cornerstone of the smart grid in China and it is being developed at an unprecedented speed. Due to its small dc resistance and limited capability of UHV transformer to withstand dc bias, the UHV grid is more sensitive to geomagnetic hazards compared to other grids.

In this paper, taking a UHV Grid in Sanhua China for example, we propose an efficient method based on the stochastic simulation tools of polynomial chaos (PC) to perform uncertainty quantification (UQ) for geo-electric fields and GICs. The earth conductivities and the dc resistances are used as input variables with proper distributions, and the output variables are the peak

Manuscript received September 25, 2018; revised December 5, 2018 and January 14, 2019; accepted January 20, 2019. This work was supported by the National Key R&D Program of China under Grant 2016YFC0800100. (*Corresponding author: Yan-zhao Xie.*)

Q. Liu is with the State Key laboratory of Power Equipment and Electrical Insulation, National Center for International Research on Transient Electromagnetics and Applications, Xi'an Jiaotong University, Xi'an 710049, China, and also with the College of Electrical and Control Engineering, Xi'an University of Science and Technology, Xi'an 710054, China (e-mail: liuqing623nn@163.com).

Y.-z. Xie, N. Dong, Y.-h. Chen, and M.-z. Liu are with the State Key laboratory of Power Equipment and Electrical Insulation, National Center for International Research on Transient Electromagnetics and Applications, Xi'an Jiaotong University, Xi'an 710049, China (e-mail: yzxie@mail.xjtu.edu.cn; dongning96@163.com; chenyuha0@stu.xjtu.edu.cn; liuminzhou@outlook.com).

Q. Li is with the School of Engineering, University of Edinburgh, EH8 9YL Edinburgh, U.K. (e-mail: quan.li@ed.ac.uk).

Color versions of one or more of the figures in this paper are available online at <http://ieeexplore.ieee.org>.

Digital Object Identifier 10.1109/TEMC.2019.2894945

80 values of the time series of geo-electric fields and GICs during  
 81 storm event. The results obtained give a clear indication of the  
 82 GIC levels of all substations and the sensitivities of GICs in  
 83 different substations to different input variables. The conclusions  
 84 will provide comprehensive and useful information for  
 85 GIC evaluation and mitigation.

## 86 II. UC MODEL OF THE GEO-ELECTRIC FIELDS AND GICs

### 87 A. Calculation Method of the Time Series of Geo-Electric 88 Fields and GIC

89 In GIC calculation, 1-D earth model is mostly adopted due to  
 90 its simplicity and acceptable accuracy. The variable conductivity  
 91 of the earth can be modeled by a series of horizontal layers  
 92 with specified conductivity and thickness. Based on the “plane  
 93 wave” method, the surface impedance  $Z_0(\omega)$  of  $m$ -layer earth  
 94 can be calculated by using the recursive relation in [10]. In the  
 95 frequency domain,  $Z_0(\omega)$  is also the transfer function between  
 96 the surface electric fields and magnetic field, the relationships  
 97 between which are

$$E_y(\omega) = -\frac{1}{\mu_0} B_x(\omega) Z_0(\sigma_1, \sigma_2, \dots, \sigma_m, h_1, h_2, \dots, h_{m-1}, \omega) \quad (1)$$

$$E_x(\omega) = \frac{1}{\mu_0} B_y(\omega) Z_0(\sigma_1, \sigma_2, \dots, \sigma_m, h_1, h_2, \dots, h_{m-1}, \omega) \quad (2)$$

98 where  $\sigma_i$  ( $i = 1, 2, \dots, m$ ) and  $h_i$  ( $i = 1, 2, \dots, m - 1$ ) are the  
 99 conductivity and thickness of each layer, and  $\omega$  is the angular  
 100 frequency.

101 The real-time magnetic field data from a magnetic observa-  
 102 tory can be converted to the frequency domain through Fourier  
 103 transform. So the electric fields in the frequency domain can  
 104 be obtained by (1) and (2). Then, by applying inverse Fourier  
 105 transform, we can get the time series of  $E_x(t)$  and  $E_y(t)$ . Due  
 106 to the insignificant error, we ignore the effect of shield wires on  
 107 geoelectric field calculation. These electric fields can be used  
 108 as an input for a power system model for every time incre-  
 109 ment to calculate the voltage sources, which drive GIC flows in  
 110 the power grid. For the transmission line from substation  $a$  to  
 111 substation  $b$ , the voltage is given by

$$V_{ab}(t) = E_x(t) \cdot L_N + E_y(t) \cdot L_E \quad (3)$$

112 where  $L_N$  is the northward distance and  $L_E$  is the eastward  
 113 distance. They are related to the latitudes and longitudes of the  
 114 two substations and can be calculated by the formulas in [18].

115 Then, GICs from substations to ground can be obtained by

$$\text{GIC} = (1 + \mathbf{YZ})^{-1} \mathbf{J} \quad (4)$$

116 which is presented by Lehtinen and Pirjola [19], where,  $\mathbf{Y}$  and  $\mathbf{Z}$   
 117 are the network admittance matrix and the earthing impedance  
 118 matrix, respectively.  $\mathbf{J}$  depends on the voltages determined by the  
 119 electric field along the transmission line and the line resistance,  
 120 for example, for the node  $b$ ,  $J_b$  is decided by

$$J_b = \sum_{b=1, b \neq a}^N \frac{V_{ba}}{R_{ba}}. \quad (5)$$

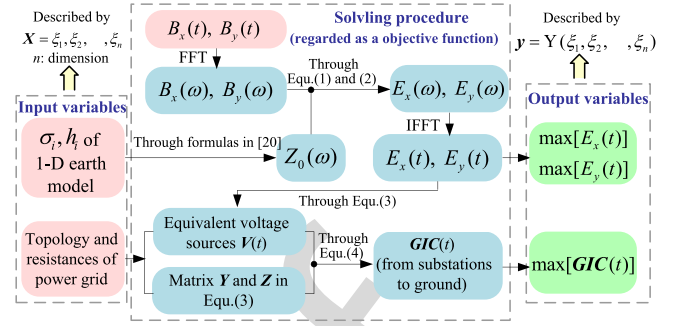


Fig. 1. Solving procedure of the maximums of geo-electric fields and GICs.

121 When the time series of geo-electric fields and GIC during a  
 122 given storm event have been calculated, we can find the max-  
 123 imums of geo-electric fields and GIC during this storm event.  
 124 The solving procedure can be presented in Fig. 1. The input  
 125 variables are described by the  $n$ -dimensional vector  $\xi$ , which  
 126 can be either the uncertain parameters of the layered earth or  
 127 the dc resistances of the power grid. In this paper, what we  
 128 are mainly concerned about, i.e., the output variables, are the  
 129 maximums of the geo-electric fields and GICs during a storm  
 130 event. For convenience, a function is used to represent the solv-  
 131 ing processing, and the output variables can be expressed by  
 132  $\mathbf{y} = \mathbf{Y}(\xi_1, \xi_2, \dots, \xi_n)$ .

### 133 B. Derivation of PC Expansions for Output Variables

134 The traditional way to analyze the uncertainty of output vari-  
 135 ables in varied input scenarios is to use the Monte Carlo (MC)  
 136 method. The first step is to sample randomly according to the  
 137 distribution type and intervals of the input variables. The sam-  
 138 ples are denoted by

$$\tilde{\mathbf{X}}^{(s)} = (\tilde{\xi}_1^{(s)}, \tilde{\xi}_2^{(s)}, \dots, \tilde{\xi}_n^{(s)}) \quad s = 1, 2, \dots, m. \quad (6)$$

139 The sample number (i.e.,  $m$ ) usually should be big enough  
 140 to obtain satisfactory results and in this paper,  $m$  is set to be  
 141 10000. Next, put the samples into the objective function, then  
 142 the outputs for all different sample sets can be calculated.

143 Although the MC method is simple and clear, its efficiency  
 144 decreases with the increasing of the sample number. Some tech-  
 145 niques can solve this problem very well [20], [21], such as PC  
 146 method. According to PC theory, the objective function can be  
 147 expanded with respect to  $\mathbf{X}$  using a series of orthogonal basis  
 148 functions. In practice, we need to truncate the order of expan-  
 149 sion to a finite order  $P$ . After truncation, the expansion can  
 150 approximate the real response

$$\mathbf{Y}(\mathbf{X}) \approx \hat{\mathbf{Y}}(\mathbf{X}) = \sum_{k=0}^P A_k \Psi_k(\mathbf{X}) \quad (7)$$

151 where  $A_k$  represent the expansion coefficients to be estimated,  
 152  $\Psi_k(\mathbf{X})$  is a class of multivariate polynomials which involve  
 153 products of the 1-D polynomials;  $k$  is the term number of the  
 154 expansion. To obtain the expansion, multivariate polynomials  
 155 and the coefficients need to be determined.

156 1) *Determination of Multivariate Polynomials:* For each input  
 157 variable, its 1-D orthogonal polynomial basis  $\psi_j(\xi_i)$  of  $j$   
 158 order can be determined by Askey scheme [22]. Then,  $\Psi_k(\mathbf{X})$   
 159 can be obtained easily by multiplying  $\psi_j(\xi_i)$ . Traditionally, the  
 160 PC expansion includes a complete basis of polynomials up to a  
 161 fixed total order. For example, the multidimensional polynomials  
 162 for a 2-order expansion over two random dimensions are

$$\begin{aligned}\Psi_0(\xi_1, \xi_2) &= \psi_0(\xi_1)\psi_0(\xi_2), \Psi_1(\xi_1, \xi_2) = \psi_1(\xi_1)\psi_0(\xi_2) \\ \Psi_2(\xi_1, \xi_2) &= \psi_0(\xi_1)\psi_1(\xi_2), \Psi_3(\xi_1, \xi_2) = \psi_2(\xi_1)\psi_0(\xi_2) \\ \Psi_4(\xi_1, \xi_2) &= \psi_1(\xi_1)\psi_1(\xi_2), \Psi_5(\xi_1, \xi_2) = \psi_0(\xi_1)\psi_2(\xi_2).\end{aligned}\quad (8)$$

163 Regarding the total-order expansion method (truncating all  
 164 the product items of 1-D polynomials to  $d$  order), the number  
 165 of the coefficients, i.e., the total number of the expansion terms  
 166 should be given by

$$Q = P + 1 = (n + d)! / (n!d!). \quad (9)$$

167 2) *Calculation of Polynomial Coefficients:* For 1-D input  
 168 variable, the coefficients can be calculated by numerical in-  
 169 tegration. But for multi-dimensional input variables, numerical  
 170 integration is no longer efficient. We use the stochastic response  
 171 surface method to calculate the coefficients. The first step is to  
 172 sample randomly from the parameter space of the input vari-  
 173 ables, which is denoted by

$$\{\tilde{\mathbf{X}}^{(s')}, s' = 1, 2, \dots, L\}, \text{ where } : \tilde{\mathbf{X}}^{(s')} = \tilde{\xi}_1^{(s')}, \tilde{\xi}_2^{(s')}, \dots, \tilde{\xi}_n^{(s')}. \quad (10)$$

174 To achieve the acceptable accuracy, the number of sample  
 175 sets (i.e.,  $L$ ) used to solve the coefficients should usually be no  
 176 less than  $2Q$ .

177 The second step is to plug these  $L$  sets of samples into the  
 178 objective functions  $Y(\mathbf{X})$  and the right-hand side of (7), respec-  
 179 tively, and then,  $L$  real responses and  $L$  approximate responses  
 180 can be obtained. The coefficients should make the approxima-  
 181 tions close to the real ones, which can be written by  $L$  equations  
 182 expressed in matrix equation

$$\begin{bmatrix} \Psi_0(\tilde{\mathbf{X}}^{(1)}) & \Psi_1(\tilde{\mathbf{X}}^{(1)}) & \dots & \Psi_P(\tilde{\mathbf{X}}^{(1)}) \\ \Psi_0(\tilde{\mathbf{X}}^{(2)}) & \Psi_1(\tilde{\mathbf{X}}^{(2)}) & \dots & \Psi_P(\tilde{\mathbf{X}}^{(2)}) \\ \vdots & \vdots & \ddots & \vdots \\ \Psi_0(\tilde{\mathbf{X}}^{(L)}) & \Psi_1(\tilde{\mathbf{X}}^{(L)}) & \dots & \Psi_P(\tilde{\mathbf{X}}^{(L)}) \end{bmatrix} \begin{bmatrix} A_0 \\ A_1 \\ \vdots \\ A_P \end{bmatrix} = \begin{bmatrix} Y(\tilde{\mathbf{X}}^{(1)}) \\ Y(\tilde{\mathbf{X}}^{(2)}) \\ \vdots \\ Y(\tilde{\mathbf{X}}^{(L)}) \end{bmatrix}. \quad (11)$$

183 Equation (11) can be simplified as

$$\mathbf{B}\mathbf{A} = \mathbf{Y} \quad (12)$$

184 Obviously, (11) is an overdetermined equation, and the co-  
 185 efficients are the solution of this equation. If matrix  $\mathbf{B}^T\mathbf{B}$  is  
 186 nonsingular, (11) has a unique solution, which can be calculated

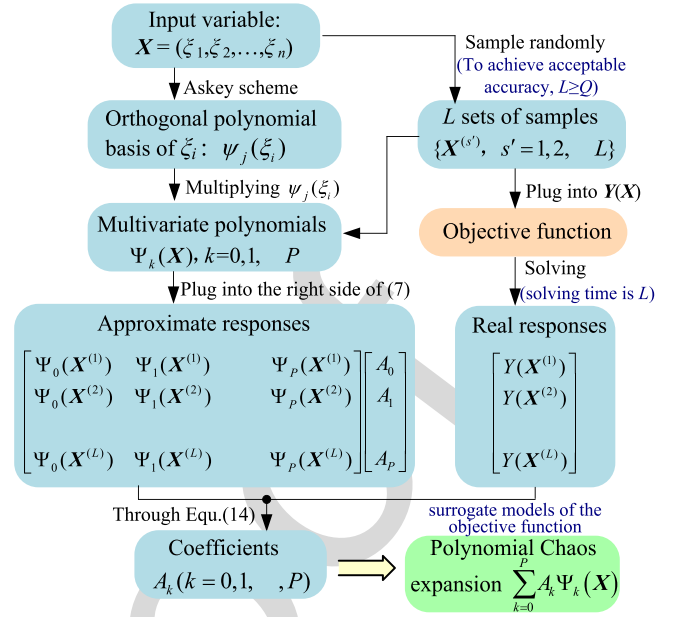


Fig. 2. Workflow of the PC method.

by (13) according to least quadratic regression

$$\hat{\mathbf{A}} = (\mathbf{B}^T\mathbf{B})^{-1}\mathbf{B}^T\mathbf{Y}. \quad (13)$$

188 The workflow of the PC method is shown in Fig. 2. Once  
 189 the coefficients are obtained, the PC expansions regarded as  
 190 surrogate models of the objective function  $Y(\mathbf{X})$  are obtained.

191 Obviously, to get the PC expansions for output variables it  
 192 only needs a few iterations to solve the objective function. Then,  
 193 we can carry out UQ with these surrogate models available,  
 194 which is much faster than running a large number of MC simu-  
 195 lations for the objective function.

### III. UQ OF GEO-ELECTRIC FIELDS AND GICS OF SANHUA GRID

#### A. Topology and Parameters of Sanhua Grid

197 Sanhua Grid is a UHV ac system in China, interconnecting  
 198 three regional power grids including North China grid, Central  
 199 China grid, and East China grid. Fig. 3 shows the geographic  
 200 location of the Sanhua Grid discussed in this paper, within which  
 201 only the level of 1000 kV is considered. The grid consists of  
 202 37 substations and 45 transmission lines. The substations are  
 203 numbered from 1 to 37, and their numbers and names are all  
 204 labeled. The transmission lines are labeled with blue numbers.  
 205

206 Calculation of GIC requires three sets of resistance param-  
 207 eters. The typical value of substation grounding resistance is  
 208  $0.1 \Omega$ , assuming all transformers are grounded directly. The  
 209 1000 kV lines are comprised of 8-bundled conductors LGJ-  
 210 500/35 per phase, and the dc resistance of every phase is  
 211  $0.0095 \Omega/\text{km}$  (at  $20^\circ\text{C}$ ), the lengths of which can be obtained  
 212 from [23] and electric power design institutes. From transformer  
 213 manufacturers, the typical values of dc resistance per phase of  
 214 the series and common winding are 182.7 and 141.5 m $\Omega$  at  
 215  $75^\circ\text{C}$ , respectively. With these parameters the equivalent circuit  
 216 of this grid can be modeled.



Fig. 3. Geographic location of the part of Sanhua 1000 kV power grid considered in this paper.

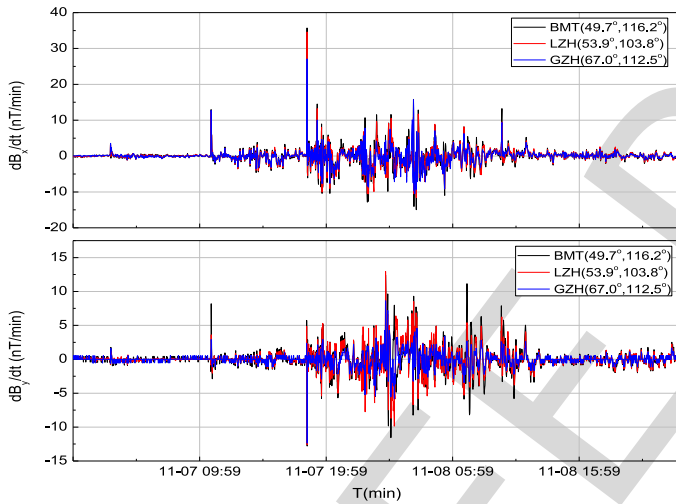


Fig. 4.  $dB/dt$  calculated from recorded magnetic-field variations at three magnetic observatories, November 7–8, 2004.

In this section, we will carry out UQ for the maximums of geo-electric fields and GICs during a storm event. As an example, a GMD event on November 7–8, 2004 was selected. The magnetic field recordings from three main magnetic observatories (marked by the red triangles in Fig. 3) starting from November 7 until the end of November 8 are obtained, which comprised 2880 data points with a sampling interval of 1 min. Magnetic derivatives against time ( $dB/dt$ ) were calculated from the magnetic field recordings that are shown in Fig. 4. It shows that the rates of magnetic field change at three observatories are almost identical. Therefore, it is reasonable and acceptable to assume the magnetic field to be uniform over the geographical area of the entire power grid. In the next calculation, the magnetic field records from BMT observatories will be used.

Based on the four-layer earth conductivity model [23] and the interpretation of existing geophysical measurements [24], [25], the ranges of the soil layer conductivities are roughly determined

TABLE I  
EFFECT OF TRUNCATION ORDER OF PC METHOD ON ERROR PERCENTAGE

$d$	Compare projects						$Q$	$L$
	Mean (%)		Standard deviation(%)		Median (%)			
	$E_x$	$E_y$	$E_x$	$E_y$	$E_x$	$E_y$		
1	5.288	0.378	23.83	14.07	10.30	2.459	5	10
2	0.261	0.012	2.627	2.382	0.476	0.016	15	30
3	0.027	0.154	2.628	3.940	0.689	0.202	35	70
4	0.061	0.013	0.390	0.767	0.071	0.129	66	132
5	0.034	0.073	0.496	1.650	0.018	0.021	126	252

Here,  $d$  is the truncation order of the PC expansions.  $Q$  is the number of polynomial terms. When we calculate the coefficients of PC expansion, we sample  $L$  (equal to  $2Q$ ) sets of samples and put them into the objective functions. So  $L$  is also the solution times to the objective function.

and their values are assumed to be of uniform distribution. Nevertheless, the uniform distribution may not be optimal, if sufficient values of soil conductivities can be acquired; then, more preferable distributions would be inferred based on Bayesian methods. Subscripts 1–4 are used to denote each layer from the top layer downwards. The thicknesses of the top three layers are 30, 60, and 60 km. The resistivity variable ranges assigned to each layer are [100, 2000], [50, 770], and [25, 2000]  $\Omega$ -m. Under a depth of 150 km, it is a bottom half-space with the resistivity from 1 to 3  $\Omega$ -m.

### B. UQ for the Maximums of Geo-Electric Fields

For geo-electric field study, the 4-D input variables are the conductivities of the four-layer earth following random distribution in their respective variable ranges. They are denoted by  $\mathbf{X} = (\xi_1, \xi_2, \xi_3, \xi_4) = (\sigma_1, \sigma_2, \sigma_3, \sigma_4)$ .

According to the distribution characteristic of input variables, 10 000 samples can be obtained and used as 10 000 input conditions. Then 10 000 outputs can be calculated either by MC method or by PC method. With these results, we can calculate the mean, standard deviation, and median of geo-electric field maximums. Taking the results of MC method as a reference, we can calculate the error percentages between the PC method and MC method. For PC method, different truncation orders have different calculation accuracies. The error percentages between two methods with different orders are compared in Table I.

It indicates that the higher the order is, the more accurate the results are. Considering that the term number and the solution time will increase along with the orders, the third order PC expansion would be appropriate. Compared with 10 000 iterations to the objective function of MC method, the third order PC method only needs to solve the objective function 70 iterations to achieve approximated accuracy.

The cumulative probability density (CDF) curves of the maximums of  $E_x$  and  $E_y$  are shown in Fig. 5, which provides the ranges of geo-electric field maximums during the storm event and the probabilities of different maximums.

### C. UQ for the Maximums of GIC

The above mentioned dc resistances of transmission lines and transformer windings are the values at specific temperatures. In

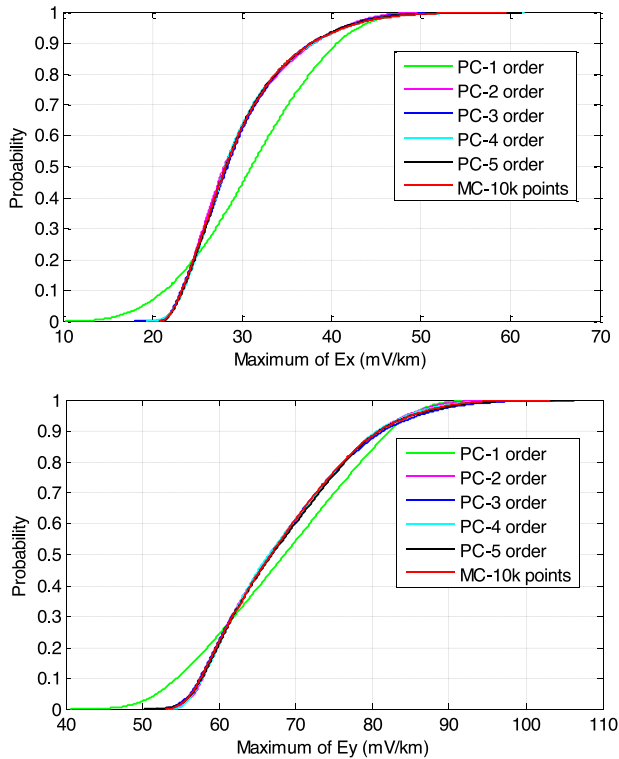


Fig. 5. Comparison of CDF of the geo-electric field maximums obtained by PC method and MC method.

273 practice, they would change with temperatures. In addition, the  
 274 product parameters of different manufacturers may be slightly  
 275 different. The grounding resistance may change with soil moisture  
 276 and corrosion situations of the grounding conductor. Hence,  
 277 for the UQ of GIC, dc resistances should be treated as input variables  
 278 as well. The input variables are therefore 7-D, which can  
 279 be expressed by the vector of  $\mathbf{X} = (\sigma_1, \sigma_2, \sigma_3, \sigma_4, R_1, R_2, R_3)$ .  
 280 Here,  $R_1$  denotes the resistance per unit length of transmission  
 281 line,  $R_2$  denotes the winding resistance, and  $R_3$  denotes the sub-  
 282 station grounding resistance. Considering the practical operation,  
 283 we roughly assume that the transmission line resistances  
 284 vary from 0.00912 to 0.0114  $\Omega/\text{km}$ , and the values of trans-  
 285 former windings range between  $\pm 8\%$ . Considering the design  
 286 requirement of grounding resistance and the practical operation  
 287 in UHV substations, the reasonable range of grounding resis-  
 288 tance is from 0.08 to 0.12  $\Omega$ . The resistance values are assumed  
 289 to follow uniform distribution.

290 Similarly, the GIC maximums of all the substations in Sanhua  
 291 grid can be obtained by using the PC method. For example, the  
 292 CDF curves of the No.1 substation computed by the MC method  
 293 and PC method under different orders are shown in Fig. 6. It  
 294 shows that the accuracy is acceptable when the order is greater  
 295 than two. The same conclusion could be derived from other  
 296 substations.

297 The number of polynomial terms and program running time  
 298 under different orders are compared in Table II. For MC method,  
 299 it takes 3 h 26 min to finish 10 000 outputs. But even for 5-order  
 300 PC expansion including 792 polynomial terms, it would take  
 301 only about half an hour to get 10 000 outputs. Obviously, the

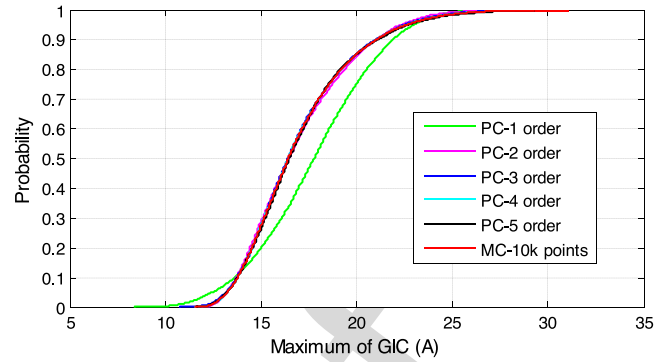


Fig. 6. Comparison of CDF curves of GIC maximums in No.1 substation calculated by PC expansions and MC method.

TABLE II  
COMPARISONS OF PC METHOD UNDER DIFFERENT ORDER

Order	1	2	3	4	5
$Q$	8	36	120	330	792
$L$	16	72	240	660	1584
$t_1$	40.068s	93.654s	4min39s	14min5s	32min24s
$t_2$	4.404s	5.630s	11.932s	34.196s	109.844s

$Q$  and  $L$  have the same meaning as those in Table I. Here,  $t_1$  is the approximate program run time to get the PC expansions, and  $t_2$  is the program run time to substitute 10 000 sample sets in the PC expansion to obtain 10 000 outputs. The main computer configuration is 8G memory and Intel i5-5200U CPU (2.2 GHz).

302 PC method can greatly shorten simulation time and increase the  
 303 computation efficiency.

304 After comprehensive comparison, we choose the 3-order PC  
 305 expansions to carry out UQ for GIC maximums. Then, we carry  
 306 out statistical analysis for the 10 000 outputs to get extra infor-  
 307 mation, such as variances, means, and cumulative probability  
 308 density. The results are shown in Fig. 7, which provides the GIC  
 309 maximums in all the 37 substations, as well as their interval  
 310 distributions. It shows that in almost half of the 37 substations,  
 311 the maximums of GIC from substation to the earth would exceed  
 312 20 A. The GIC in the Jingwest substation and the Shanghai  
 313 substation are larger than the others due to the “edge effect.”

314 Similarly, the CDF of all output variables could be calculated.  
 315 Due to limited space, only the CDF curves and histograms of 12  
 316 crucial substations are listed in Fig. 8. The information provided  
 317 by Fig. 8 could clarify the distribution characteristics of GIC  
 318 maximums and how frequently the values may occur.

319 Obviously, for each input sample, there is a corresponding  
 320 output. And among these outputs, we can find the condition  
 321 under which the highest GIC maximums would appear. For  
 322 example, GIC time series in three substations are shown in  
 323 Fig. 9. The horizontal coordinate donates the time with the unit  
 324 of minutes. The red texts are the values of GIC maximums  
 325 during this storm event.

#### IV. SENSITIVITY STUDIES

326  
 327 The sensitivity analysis based on variance decomposition can  
 328 be used to quantify the influence of the input variables on the  
 329 output variables.

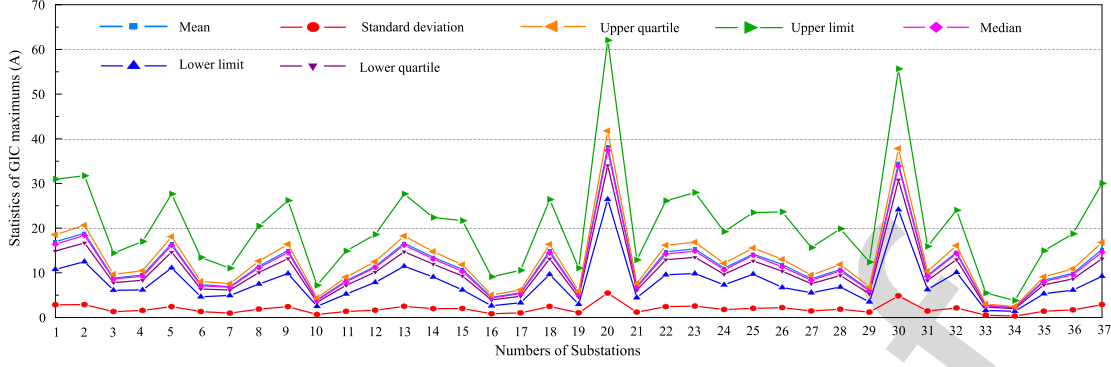


Fig. 7. Comparison of seven kinds of statistic parameters of GIC maximums in 37 substations.

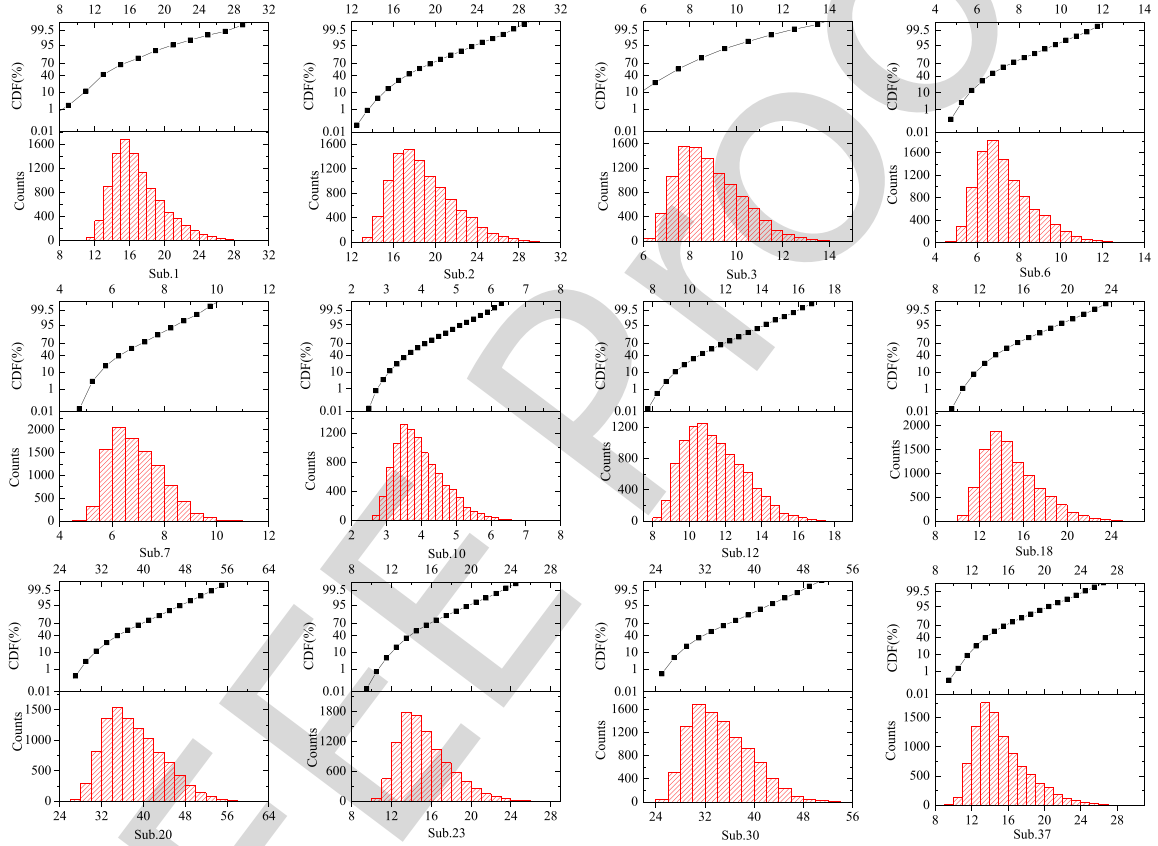


Fig. 8. Cumulative probability density curves and histograms of 12 crucial substations. The horizontal axis denotes the maximum of GIC with the unit of ampere. The numbers of substations are labeled below the graph.

330 The variance of the objective function and the partial vari-  
 331 ances of single input variable or between input variables are  
 332 denoted by  $V$  and  $V_{i_1, i_2, \dots, i_s}$ , respectively. The Sobol indices  $S_i$   
 333 and the total Sobol indices  $S_i^T$  of the response  $Y(\mathbf{X})$  with respect  
 334 to the input variables  $x_i$  are as follows [26]:

$$S_{i_1, \dots, i_s} = \frac{V_{i_1, \dots, i_s}}{V} \quad 1 \leq i_1 < \dots < i_s \leq n; \quad s = 1, 2, \dots, n$$

$$S_i^T = \sum_{\tau_i} S_{i_1, \dots, i_s}, \quad \tau_i = \{(i_1, \dots, i_s) : \exists k, 1 \leq k \leq s, i_k = i\}.$$

For  $d$ -order PC expansion, the total Sobol indices can be  
 335 estimated by  
 336

$$S_i^T = \frac{\sum \gamma_i A_{i_1, \dots, i_t}^2}{V}, \quad \gamma_i = \{(i_1, \dots, i_t) : \exists k, 1 \leq k \leq t, i_k = i\}$$

$$1 \leq i_1 < \dots < i_t \leq n; \quad t = 1, 2, \dots, d.$$

$$(14) \quad V = \sum_{i_1=1}^n A_{i_1}^2 + \sum_{i_1=1}^n \dots \sum_{i_d=1}^{i_{d-1}} A_{i_1, i_2, \dots, i_d}^2. \quad (16)$$

In order to illustrate the effects of all input random variables  
 337 mentioned previously on the output variables, we calculate the  
 338

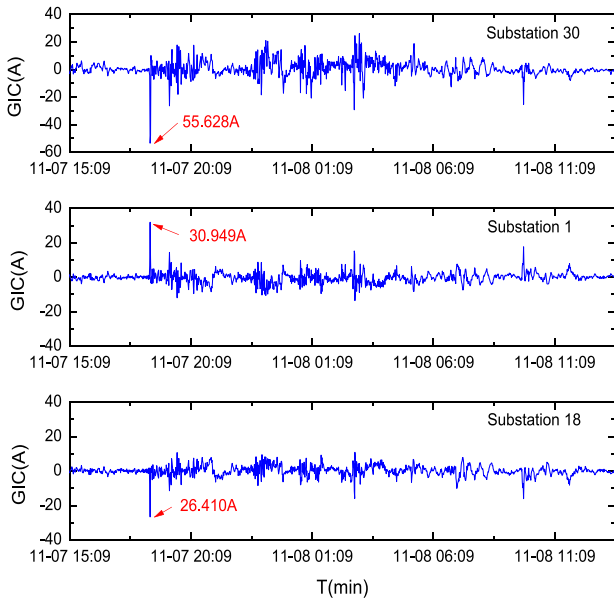


Fig. 9. Time series of GICs in three substations.

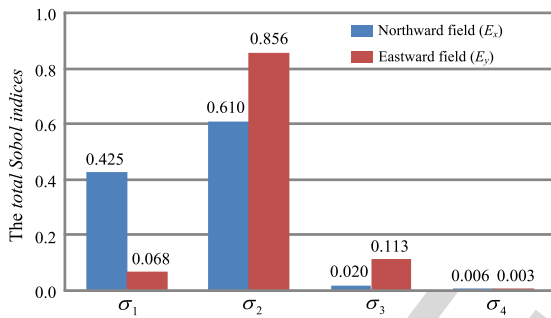


Fig. 10. Total Sobol indices of the maximums of geo-electric fields.  $\sigma_1$ ,  $\sigma_2$ ,  $\sigma_3$ , and  $\sigma_4$  are the earth conductivities of the four-layer model, respectively.

total Sobol indices with the coefficients solved above. The total Sobol indices of the maximums of geo-electric fields to the earth conductivities are presented in Fig. 10.

Regarding the example studied in this paper, it shows that the northward field is mainly related to the conductivities of the top two layers, and the eastward field is more sensitive to the conductivity of the second layer. The earth conductivity below 150 km has little effect on geo-electric fields.

The same work can be done for the GICs from substation to the ground. In Fig. 11, for the given distribution characteristics of the input variables in this paper, we list the total Sobol indices of the 12 substations considered in Section III. Obviously, the GIC maximums are more sensitive to earth conductivities than the resistances, especially to the conductivity of the second layer. The influence of the 7-D input variables on different substations is mainly due to their different geographic locations as well as their relative positions within the grid.

### V. CONCLUSION

In this paper, considering the complex and uncertain input parameters in GIC calculation, we propose an UQ model of the



Fig. 11. Total Sobol indices of the maximums of GICs in 12 substations.

geo-electric fields and GICs. The UQ for the geo-electric fields and GICs of a UHV power grid is carried out.

The PC expansion provides an efficient surrogate model to replace the objective function which can be used to analyze the uncertainty of the origin problem easily. For the calculation of GIC under 10 000 sample sets, the computational time of the PC method takes only one fortieth of that of the MC method.

For the considered storm event, the northward fields and eastward fields vary from 18.654 to 55.791 mV/km and from 51.864 to 103.416 mV/km, respectively. In all the substations within the grid, 17 stations experience GICs exceeding 20 A in amplitude. GIC levels of some substations are relatively higher than others, especially substations No.20 and No.30.

The total Sobol indices are calculated by using the PC expansion coefficients. Sensitivity analysis shows that, the conductivity of the second layer has a greater impact on the geo-electric fields and GICs than the other layers. In different substations, the GICs are sensitive to their geological locations involving the 7-D input variables. Sufficient consideration should be given to the grounding resistance of substations when carrying out GIC evaluation and mitigation.

The proposed method can effectively offer a better understanding of the sensitivities of GICs to input uncertain variables and give a reasonable evaluation of the geomagnetic hazards to the power system. In the future, we will strive to acquire more information to set up an exact earth conductivity model for GIC UQ. Furthermore, we will monitor the substations where the GIC levels are relatively high in order to validate the computational model that makes it possible to provide predicted GIC based on the correlative predicted data of space weather.

### ACKNOWLEDGMENT

The authors would like to thank the electric power design institutes for providing certain parameters of the Sanhua grid and Prof. S.-m. Wang for the useful advice on earth model.



## REFERENCES

- [1] D. H. Boteler, R. Pirjola, and H. Nevanlinna, "The effects of geomagnetic disturbances on electrical systems at the Earth's surface," *Adv. Space Res.*, vol. 22, no. 1, pp. 17–27, Sep. 1998.
- [2] R. Pirjola, "Geomagnetically induced currents during magnetic storms," *IEEE Trans. Plasma Sci.*, vol. 28, no. 6, pp. 1867–1873, Dec. 2000.
- [3] L. Bolduc, P. Langlois, and D. Boteler, "A study of geoelectromagnetic disturbances in Québec, 2. Detailed analysis of a large event," *IEEE Trans. Power Del.*, vol. 15, no. 1, pp. 272–278, Feb. 2000.
- [4] D. Boteler, R. Pirjola, A. Viljanen, and O. Amm, "Prediction of geomagnetically induced currents in power transmission system," *Adv. Space Res.*, vol. 26, no. 1, pp. 5–14, Mar. 2000.
- [5] V. V. Vakhnina, V. A. Shapovalov, V. N. Kuznetsov, and D. A. Kretov, "The influence of geomagnetic storms on thermal processes in the tank of a power transformer," *IEEE Trans. Power Del.*, vol. 30, no. 4, pp. 1702–1707, Aug. 2015.
- [6] W. A. Radasky, "Impacts of variations of geomagnetic storm disturbances on high voltage power systems," *IEEE Trans. Power Energy*, vol. 133, no. 12, pp. 931–934, Dec. 2013.
- [7] C. Barbosa, G. Hartmann, and K. Pinheiro, "Numerical modeling of geomagnetically induced currents in a Brazilian transmission line," *Adv. Space Res.*, vol. 55, no. 4, pp. 1168–1179, Nov. 2015.
- [8] Q. Liu, K. Han, and Y. Bai, "Analysis of distribution regularities and sensitivity of geomagnetically induced currents in planned Xinjiang 750 kV power grid," *Power Syst. Technol.*, vol. 41, no. 17, pp. 3678–3684, Nov. 2017.
- [9] R. Pirjola, "Review on the calculation of surface electric and magnetic fields and of GICs in ground based technological systems," *Surv. Geophys.*, vol. 23, no. 1, pp. 71–90, Jan. 2002.
- [10] D. Boteler, "The use of linear superposition in modelling geomagnetically induced currents," in *Proc. IEEE Power Energy Soc. General Meeting*, 2013, pp. 1–5.
- [11] D. H. Boteler, "The evolution of québec earth models used to model geomagnetically induced currents," *IEEE Trans. Power Del.*, vol. 30, no. 5, pp. 2171–2178, Oct. 2015.
- [12] L. Marti, C. Yiu, A. Rezaei-Zare, and D. Boteler, "Simulation of geomagnetically induced currents with piecewise layered-earth models," *IEEE Trans. Power Del.*, vol. 29, no. 4, pp. 1886–1893, Aug. 2014.
- [13] J. L. Gilbert, "Simplified techniques for treating the ocean-land interface for geomagnetically induced electric fields," *IEEE Trans. Electromagn. Compat.*, vol. 57, no. 4, pp. 688–692, Aug. 2015.
- [14] J. J. Love, G. M. Lucas, A. Kelbert, and P. A. Bedrosian, "Geoelectric hazard maps for the mid-atlantic united states: 100 year extreme values and the 1989 magnetic storm," *Geophys. Res. Lett.*, vol. 45, no. 1, pp. 5–14, Jan. 2018.
- [15] H. Karami *et al.*, "Effect of mixed propagation path on electromagnetic fields at ground surface produced by electrojet," *IEEE Trans. Electromagn. Compat.*, vol. 60, no. 6, pp. 2019–2024, Dec. 2018.
- [16] X. B. Chen, Q. T. Lu, and K. Zhang, "Review of magnetotelluric data inversion methods," *Prog. Geophys.*, vol. 26, no. 5, pp. 1607–1619, Oct. 2011.
- [17] V. D. Albertson, J. G. Kappenman, and N. Mohan, "Load-flow studies in the presence of geomagnetically-induced currents," *IEEE Trans. Power App. Syst.*, vol. PAS-100, no. 2, pp. 594–607, Feb. 1981.
- [18] R. Horton, D. Boteler, T. J. Overbye, R. Pirjola, and R. C. Dugan, "A test case for the calculation of geomagnetically induced currents," *IEEE Trans. Power Del.*, vol. 27, no. 4, pp. 2368–2373, Oct. 2012.
- [19] M. Lehtinen and R. Pirjola, "Currents produced in earthed conductor networks by geomagnetically induced electric fields," *Annales Geophysicae*, vol. 3, no. 4, pp. 479–484, Jan. 1985.
- [20] Z. Fei, Y. Huang, J. Zhou, and Q. Xu, "Uncertainty quantification of crosstalk using stochastic reduced order models," *IEEE Trans. Electromagn. Compat.*, vol. 59, no. 1, pp. 228–239, Feb. 2017.
- [21] S. Oladshkin and W. Nowak, "Data-driven uncertainty quantification using the arbitrary polynomial chaos expansion," *Rel. Eng. Syst. Safety*, vol. 106, no. 4, pp. 179–190, May 2012.
- [22] D. Xiu and G. E. Karniadakis, "The Wiener–Askey polynomial chaos for stochastic differential equations," *SIAM J. Sci. Comput.*, vol. 24, no. 2, pp. 619–644, Oct. 2002.
- [23] K. Zheng, "Research on influence factors and modelling methods of geomagnetically induced currents in large power grid," *Ph.D. dissertation*, North China Elect. Power Univ., Beijing, China, 2014.
- [24] W. Wei *et al.*, "Geoelectric structure of lithosphere beneath eastern North China: Features of a thinned lithosphere from magnetotelluric soundings," *Earth Sci. Frontiers*, vol. 15, no. 4, pp. 204–216, Jul. 2008.

- [25] Y. Liu and Y. Xu, "Lithospheric electrical characteristic in South China and its geodynamic implication," *Chin. J. Geophys.*, vol. 56, no. 12, pp. 204–216, Dec. 2013.
- [26] I. M. Sobol, "Global sensitivity indices for nonlinear mathematical models and their Monte Carlo estimates," *Math. Comput. Simul.*, vol. 55, no. 1/3, pp. 271–280, Feb. 2001.



**Qing Liu** was born in 1978. She received the B.Sc. and M.S. degrees in electrical engineering from Chongqing University, Chongqing, China, in 2000, and Xi'an Jiaotong University, Xi'an, China, in 2005, respectively. She is currently working toward the Ph.D. degree in electrical engineering at Xi'an Jiaotong University.

She is also an Associate Professor with the Xi'an University of Science and Technology, Xi'an, China. Her research interest includes modeling and assessing geomagnetically induced currents in power grids.



**Yan-zhao Xie (M'12)** was born in 1973. He received the Ph.D. degree in electrical engineering from Tsinghua University, Beijing, China, in 2005.

Since 2016, he is the Director of the National Center for International Research on Transient Electromagnetics and Applications. He is currently a Professor with Xi'an Jiaotong University, Xi'an, China. His research interests include electromagnetic transients in power system, electromagnetic compatibility, etc.



**Ning Dong** received the B.Sc. degree in electrical engineering from Xi'an Jiaotong University, Xi'an, China, in 2016. She is currently working toward the Ph.D. degree at Xi'an Jiaotong University.

Her research interest includes modeling and UC of multiconductor transmission lines coupling.



**Yu-hao Chen** received the B.Sc. degree in electrical engineering from Xi'an Jiaotong University, Xi'an, China, in 2015, where he is currently working toward the Ph.D. degree in electrical engineering.

His research interest is the effect evaluation of electromagnetic environments.



**Min-zhou Liu** received the B.Sc. degree in electrical engineering from Xi'an Jiaotong University, Xi'an, China, in 2017, where he is currently working toward the M.S. degree.

His research interests include the effect evaluation of electromagnetic environments and reliability evaluation of power system.



**Quan Li** is a Tenure Lecturer with the University of Edinburgh, Edinburgh, U.K., and Theme Leader of Applied Superconductivity.

His research interests include electromagnetism and superconducting applications in energy and healthcare sectors.

Dr. Li is a Fellow of the Higher Education Academy.

474  
475  
476  
477  
478  
479  
480  
481  
482  
483  
484  
485  
486  
487  
488  
489  
490  
491  
492  
493  
494  
495  
496  
497  
498  
499  
500  
501  
502  
503  
504  
505  
506  
507  
508  
509  
510  
511  
512  
513  
514  
515  
516  
517  
518  
519  
520  
521  
522  
523  
524  
525  
526

# Uncertainty Quantification of Geo-Magnetically Induced Currents in UHV Power Grid

Qing Liu , Yan-zhao Xie , *Member, IEEE*, Ning Dong, Yu-hao Chen, Min-zhou Liu, and Quan Li 

**Abstract**—Geo-magnetically induced currents (GICs) have attracted more attention since many Ultra-High Voltage (UHV) transmission lines have been built, or are going to be built in the world. However, when calculating GICs based on the classical model, some input parameters, such as the earth conductivity and dc resistances of the grid, are uncertain or very hard to be determined in advance. Taking this into account, the uncertainty quantification (UQ) model of the geo-electric fields and GICs is proposed in this paper. The UQ of the maximums of the geo-electric fields and GICs during storms is carried out based on the polynomial chaos (PC) method. The results of the UHV grid, 1000 kV Sanhua Grid, were presented and compared to the Monte Carlo method. The total Sobol indices are calculated by using the PC expansion coefficients. The sensitivities of geo-electric fields and GICs to the input variables are analyzed based on the total Sobol indices. Results show that the GICs and geo-electric fields can be effectively simulated by the proposed model, which may offer a better understanding of the sensitivities to input uncertain variables and further give a reasonable evaluation of the geomagnetic threat to the grid.

**Index Terms**—Geo-electric fields, Geo-magnetically induced currents (GIC), polynomial chaos (PC), total Sobol indices, uncertainty quantification (UQ).

## I. INTRODUCTION

SOLAR activities, especially coronal mass ejections, solar flares, and energetic particles, are the major factors that affect space weather and trigger geomagnetic disturbances (GMDs). The GMDs can induce low-frequency currents into power networks, known as geo-magnetically induced currents (GICs) [1]–[3]. The GICs may cause half-cycle saturation in

Manuscript received September 25, 2018; revised December 5, 2018 and January 14, 2019; accepted January 20, 2019. This work was supported by the National Key R&D Program of China under Grant 2016YFC0800100. (*Corresponding author: Yan-zhao Xie.*)

Q. Liu is with the State Key laboratory of Power Equipment and Electrical Insulation, National Center for International Research on Transient Electromagnetics and Applications, Xi'an Jiaotong University, Xi'an 710049, China, and also with the College of Electrical and Control Engineering, Xi'an University of Science and Technology, Xi'an 710054, China (e-mail: liuqing623nn@163.com).

Y.-z. Xie, N. Dong, Y.-h. Chen, and M.-z. Liu are with the State Key laboratory of Power Equipment and Electrical Insulation, National Center for International Research on Transient Electromagnetics and Applications, Xi'an Jiaotong University, Xi'an 710049, China (e-mail: yzxie@mail.xjtu.edu.cn; dongning96@163.com; chen\_yuhao@stu.xjtu.edu.cn; liuminzhou@outlook.com).

Q. Li is with the School of Engineering, University of Edinburgh, EH8 9YL Edinburgh, U.K. (e-mail: quan.li@ed.ac.uk).

Color versions of one or more of the figures in this paper are available online at <http://ieeexplore.ieee.org>.

Digital Object Identifier 10.1109/TEM.2019.2894945

power transformers, produce harmonics, and increase reactive power demand and transformer spot heat. This can lead to serious problems, such as transformer damage, voltage dips, relay disoperation, and system instability [4]–[6]. Although GMDs are more likely to happen in high latitudes, recently the phenomenon caused by GICs are also found in middle and low latitudes [7], [8], such as South Africa, Brazil, and China, which attracts broad attention.

GIC calculation requires the induced geo-electric fields over the earth's surface. The "source" of this geo-electric field (i.e., the magnetosphere-ionosphere currents) can be approximately determined by an infinite line current, surface current, or three-dimensional (3-D) current model. There are a number of methods based on different assumptions and simplifications that can be used to calculate the geo-electric fields and the GICs. A simple way is to apply an equivalent downward-propagating plane wave and assume that the earth is either uniform or layered [9]. A lot of work on geo-electric fields and GICs has been reported with specific parameters [10]–[15].

However, some input parameters are difficult to be precisely quantified, particularly in large scale power systems. For example, the earth conductivity along the depth of several hundred kilometers is an approximation of the actual structure due to the multiplicity on magnetotelluric inversion and noise interference [16]. Since the frequency of geo-electromagnetic variations is far less than that of electric power, the resistances play a dominant role for GIC calculation and the power grid can approximately be equivalent to a dc network [17]. For GIC calculation, the dynamic characteristics of ac voltages and transformer saturation should be taken into consideration. As an engineering approach, nevertheless, to model the network as resistances is more acceptable. The dc resistances of transmission lines and the transformer windings should be regarded as variables due to their changes with temperatures and should be taken into consideration.

The Ultra-High Voltage power grid is the cornerstone of the smart grid in China and it is being developed at an unprecedented speed. Due to its small dc resistance and limited capability of UHV transformer to withstand dc bias, the UHV grid is more sensitive to geomagnetic hazards compared to other grids.

In this paper, taking a UHV Grid in Sanhua China for example, we propose an efficient method based on the stochastic simulation tools of polynomial chaos (PC) to perform uncertainty quantification (UQ) for geo-electric fields and GICs. The earth conductivities and the dc resistances are used as input variables with proper distributions, and the output variables are the peak

80 values of the time series of geo-electric fields and GICs during  
 81 storm event. The results obtained give a clear indication of the  
 82 GIC levels of all substations and the sensitivities of GICs in  
 83 different substations to different input variables. The conclusions  
 84 will provide comprehensive and useful information for  
 85 GIC evaluation and mitigation.

## 86 II. UC MODEL OF THE GEO-ELECTRIC FIELDS AND GICs

### 87 A. Calculation Method of the Time Series of Geo-Electric 88 Fields and GIC

89 In GIC calculation, 1-D earth model is mostly adopted due to  
 90 its simplicity and acceptable accuracy. The variable conductivity  
 91 of the earth can be modeled by a series of horizontal layers  
 92 with specified conductivity and thickness. Based on the “plane  
 93 wave” method, the surface impedance  $Z_0(\omega)$  of  $m$ -layer earth  
 94 can be calculated by using the recursive relation in [10]. In the  
 95 frequency domain,  $Z_0(\omega)$  is also the transfer function between  
 96 the surface electric fields and magnetic field, the relationships  
 97 between which are

$$E_y(\omega) = -\frac{1}{\mu_0} B_x(\omega) Z_0(\sigma_1, \sigma_2, \dots, \sigma_m, h_1, h_2, \dots, h_{m-1}, \omega) \quad (1)$$

$$E_x(\omega) = \frac{1}{\mu_0} B_y(\omega) Z_0(\sigma_1, \sigma_2, \dots, \sigma_m, h_1, h_2, \dots, h_{m-1}, \omega) \quad (2)$$

98 where  $\sigma_i$  ( $i = 1, 2, \dots, m$ ) and  $h_i$  ( $i = 1, 2, \dots, m - 1$ ) are the  
 99 conductivity and thickness of each layer, and  $\omega$  is the angular  
 100 frequency.

101 The real-time magnetic field data from a magnetic observa-  
 102 tory can be converted to the frequency domain through Fourier  
 103 transform. So the electric fields in the frequency domain can  
 104 be obtained by (1) and (2). Then, by applying inverse Fourier  
 105 transform, we can get the time series of  $E_x(t)$  and  $E_y(t)$ . Due  
 106 to the insignificant error, we ignore the effect of shield wires on  
 107 geoelectric field calculation. These electric fields can be used  
 108 as an input for a power system model for every time incre-  
 109 ment to calculate the voltage sources, which drive GIC flows in  
 110 the power grid. For the transmission line from substation  $a$  to  
 111 substation  $b$ , the voltage is given by

$$V_{ab}(t) = E_x(t) \cdot L_N + E_y(t) \cdot L_E \quad (3)$$

112 where  $L_N$  is the northward distance and  $L_E$  is the eastward  
 113 distance. They are related to the latitudes and longitudes of the  
 114 two substations and can be calculated by the formulas in [18].

115 Then, GICs from substations to ground can be obtained by

$$\text{GIC} = (1 + \mathbf{YZ})^{-1} \mathbf{J} \quad (4)$$

116 which is presented by Lehtinen and Pirjola [19], where,  $\mathbf{Y}$  and  $\mathbf{Z}$   
 117 are the network admittance matrix and the earthing impedance  
 118 matrix, respectively.  $\mathbf{J}$  depends on the voltages determined by the  
 119 electric field along the transmission line and the line resistance,  
 120 for example, for the node  $b$ ,  $J_b$  is decided by

$$J_b = \sum_{b=1, b \neq a}^N \frac{V_{ba}}{R_{ba}}. \quad (5)$$

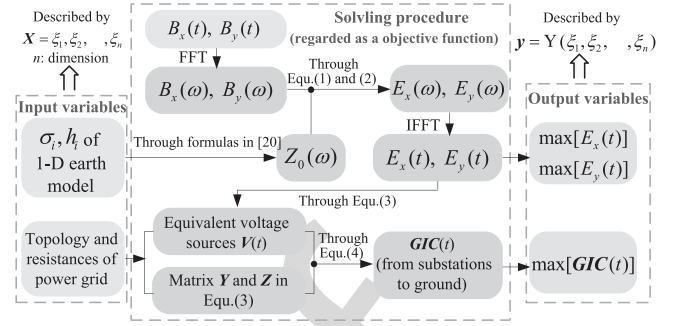


Fig. 1. Solving procedure of the maximums of geo-electric fields and GICs.

When the time series of geo-electric fields and GIC during a  
 given storm event have been calculated, we can find the max-  
 imums of geo-electric fields and GIC during this storm event.  
 The solving procedure can be presented in Fig. 1. The input  
 variables are described by the  $n$ -dimensional vector  $\xi$ , which  
 can be either the uncertain parameters of the layered earth or  
 the dc resistances of the power grid. In this paper, what we  
 are mainly concerned about, i.e., the output variables, are the  
 maximums of the geo-electric fields and GICs during a storm  
 event. For convenience, a function is used to represent the solv-  
 ing processing, and the output variables can be expressed by  
 $y = Y(\xi_1, \xi_2, \dots, \xi_n)$ .

### B. Derivation of PC Expansions for Output Variables

The traditional way to analyze the uncertainty of output vari-  
 ables in varied input scenarios is to use the Monte Carlo (MC)  
 method. The first step is to sample randomly according to the  
 distribution type and intervals of the input variables. The sam-  
 ples are denoted by

$$\tilde{X}^{(s)} = (\tilde{\xi}_1^{(s)}, \tilde{\xi}_2^{(s)}, \dots, \tilde{\xi}_n^{(s)}) \quad s = 1, 2, \dots, m. \quad (6)$$

The sample number (i.e.,  $m$ ) usually should be big enough  
 to obtain satisfactory results and in this paper,  $m$  is set to be  
 10000. Next, put the samples into the objective function, then  
 the outputs for all different sample sets can be calculated.

Although the MC method is simple and clear, its efficiency  
 decreases with the increasing of the sample number. Some tech-  
 niques can solve this problem very well [20], [21], such as PC  
 method. According to PC theory, the objective function can be  
 expanded with respect to  $X$  using a series of orthogonal basis  
 functions. In practice, we need to truncate the order of expan-  
 sion to a finite order  $P$ . After truncation, the expansion can  
 approximate the real response

$$Y(X) \approx \hat{Y}(X) = \sum_{k=0}^P A_k \Psi_k(X) \quad (7)$$

where  $A_k$  represent the expansion coefficients to be estimated,  
 $\Psi_k(X)$  is a class of multivariate polynomials which involve  
 products of the 1-D polynomials;  $k$  is the term number of the  
 expansion. To obtain the expansion, multivariate polynomials  
 and the coefficients need to be determined.

156 1) *Determination of Multivariate Polynomials:* For each input  
 157 variable, its 1-D orthogonal polynomial basis  $\psi_j(\xi_i)$  of  $j$   
 158 order can be determined by Askey scheme [22]. Then,  $\Psi_k(\mathbf{X})$   
 159 can be obtained easily by multiplying  $\psi_j(\xi_i)$ . Traditionally, the  
 160 PC expansion includes a complete basis of polynomials up to a  
 161 fixed total order. For example, the multidimensional polynomials  
 162 for a 2-order expansion over two random dimensions are

$$\begin{aligned}\Psi_0(\xi_1, \xi_2) &= \psi_0(\xi_1)\psi_0(\xi_2), \Psi_1(\xi_1, \xi_2) = \psi_1(\xi_1)\psi_0(\xi_2) \\ \Psi_2(\xi_1, \xi_2) &= \psi_0(\xi_1)\psi_1(\xi_2), \Psi_3(\xi_1, \xi_2) = \psi_2(\xi_1)\psi_0(\xi_2) \\ \Psi_4(\xi_1, \xi_2) &= \psi_1(\xi_1)\psi_1(\xi_2), \Psi_5(\xi_1, \xi_2) = \psi_0(\xi_1)\psi_2(\xi_2).\end{aligned}\quad (8)$$

163 Regarding the total-order expansion method (truncating all  
 164 the product items of 1-D polynomials to  $d$  order), the number  
 165 of the coefficients, i.e., the total number of the expansion terms  
 166 should be given by

$$Q = P + 1 = (n + d)! / (n!d!). \quad (9)$$

167 2) *Calculation of Polynomial Coefficients:* For 1-D input  
 168 variable, the coefficients can be calculated by numerical in-  
 169 tegration. But for multi-dimensional input variables, numerical  
 170 integration is no longer efficient. We use the stochastic response  
 171 surface method to calculate the coefficients. The first step is to  
 172 sample randomly from the parameter space of the input vari-  
 173 ables, which is denoted by

$$\{\tilde{\mathbf{X}}^{(s')}, s' = 1, 2, \dots, L\}, \text{ where } : \tilde{\mathbf{X}}^{(s')} = \tilde{\xi}_1^{(s')}, \tilde{\xi}_2^{(s')}, \dots, \tilde{\xi}_n^{(s')}. \quad (10)$$

174 To achieve the acceptable accuracy, the number of sample  
 175 sets (i.e.,  $L$ ) used to solve the coefficients should usually be no  
 176 less than  $2Q$ .

177 The second step is to plug these  $L$  sets of samples into the  
 178 objective functions  $Y(\mathbf{X})$  and the right-hand side of (7), respec-  
 179 tively, and then,  $L$  real responses and  $L$  approximate responses  
 180 can be obtained. The coefficients should make the approxima-  
 181 tions close to the real ones, which can be written by  $L$  equations  
 182 expressed in matrix equation

$$\begin{aligned} & \begin{bmatrix} \Psi_0(\tilde{\mathbf{X}}^{(1)}) & \Psi_1(\tilde{\mathbf{X}}^{(1)}) & \dots & \Psi_P(\tilde{\mathbf{X}}^{(1)}) \\ \Psi_0(\tilde{\mathbf{X}}^{(2)}) & \Psi_1(\tilde{\mathbf{X}}^{(2)}) & \dots & \Psi_P(\tilde{\mathbf{X}}^{(2)}) \\ \vdots & \vdots & \ddots & \vdots \\ \Psi_0(\tilde{\mathbf{X}}^{(L)}) & \Psi_1(\tilde{\mathbf{X}}^{(L)}) & \dots & \Psi_P(\tilde{\mathbf{X}}^{(L)}) \end{bmatrix} \begin{bmatrix} A_0 \\ A_1 \\ \vdots \\ A_P \end{bmatrix} \\ &= \begin{bmatrix} Y(\tilde{\mathbf{X}}^{(1)}) \\ Y(\tilde{\mathbf{X}}^{(2)}) \\ \vdots \\ Y(\tilde{\mathbf{X}}^{(L)}) \end{bmatrix}. \end{aligned} \quad (11)$$

183 Equation (11) can be simplified as

$$\mathbf{B}\mathbf{A} = \mathbf{Y} \quad (12)$$

184 Obviously, (11) is an overdetermined equation, and the co-  
 185 efficients are the solution of this equation. If matrix  $\mathbf{B}^T\mathbf{B}$  is  
 186 nonsingular, (11) has a unique solution, which can be calculated

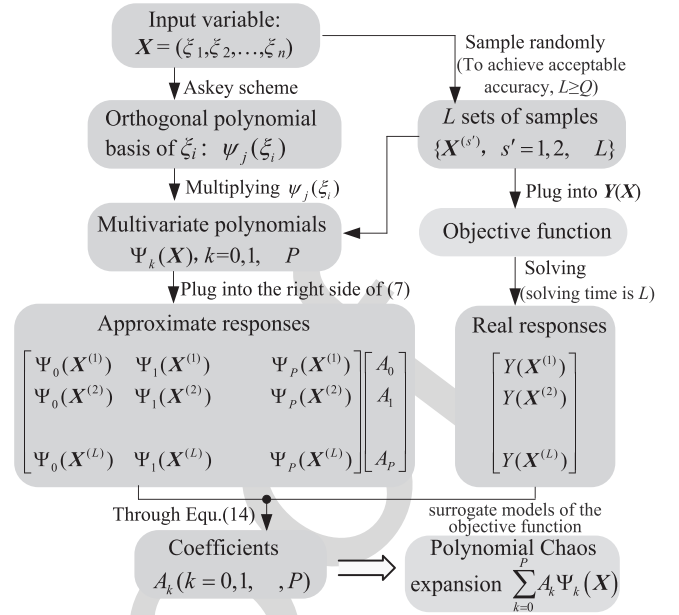


Fig. 2. Workflow of the PC method.

by (13) according to least quadratic regression

$$\hat{\mathbf{A}} = (\mathbf{B}^T\mathbf{B})^{-1}\mathbf{B}^T\mathbf{Y}. \quad (13)$$

The workflow of the PC method is shown in Fig. 2. Once  
 the coefficients are obtained, the PC expansions regarded as  
 surrogate models of the objective function  $Y(\mathbf{X})$  are obtained.

Obviously, to get the PC expansions for output variables it  
 only needs a few iterations to solve the objective function. Then,  
 we can carry out UQ with these surrogate models available,  
 which is much faster than running a large number of MC simu-  
 lations for the objective function.

### III. UQ OF GEO-ELECTRIC FIELDS AND GICS OF SANHUA GRID

#### A. Topology and Parameters of Sanhua Grid

Sanhua Grid is a UHV ac system in China, interconnecting  
 three regional power grids including North China grid, Central  
 China grid, and East China grid. Fig. 3 shows the geographic  
 location of the Sanhua Grid discussed in this paper, within which  
 only the level of 1000 kV is considered. The grid consists of  
 37 substations and 45 transmission lines. The substations are  
 numbered from 1 to 37, and their numbers and names are all  
 labeled. The transmission lines are labeled with blue numbers.

Calculation of GIC requires three sets of resistance param-  
 eters. The typical value of substation grounding resistance is  
 0.1  $\Omega$ , assuming all transformers are grounded directly. The  
 1000 kV lines are comprised of 8-bundled conductors LGJ-  
 500/35 per phase, and the dc resistance of every phase is  
 0.0095  $\Omega/\text{km}$  (at 20  $^\circ\text{C}$ ), the lengths of which can be obtained  
 from [23] and electric power design institutes. From transformer  
 manufacturers, the typical values of dc resistance per phase of  
 the series and common winding are 182.7 and 141.5 m $\Omega$  at  
 75  $^\circ\text{C}$ , respectively. With these parameters the equivalent circuit  
 of this grid can be modeled.

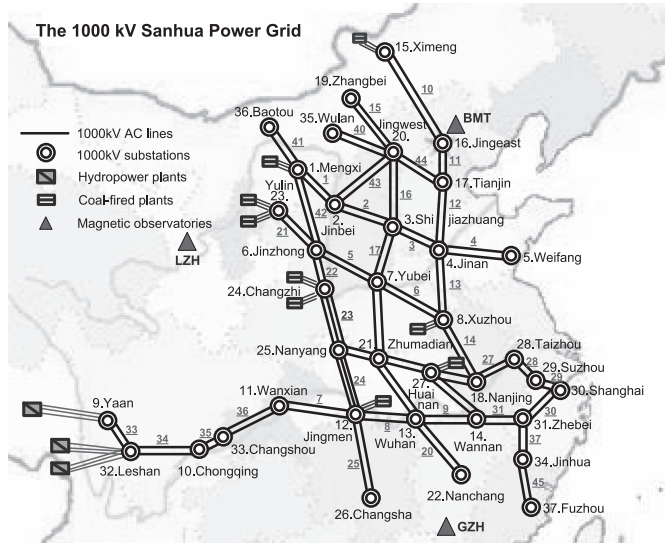


Fig. 3. Geographic location of the part of Sanhua 1000 kV power grid considered in this paper.

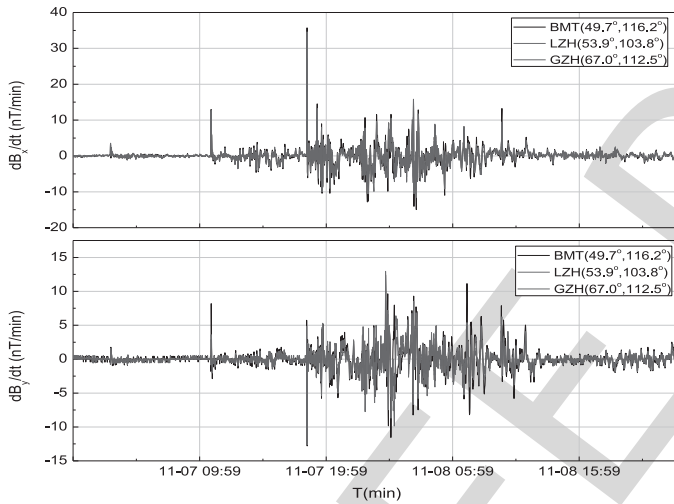


Fig. 4.  $dB/dt$  calculated from recorded magnetic-field variations at three magnetic observatories, November 7–8, 2004.

In this section, we will carry out UQ for the maximums of geo-electric fields and GICs during a storm event. As an example, a GMD event on November 7–8, 2004 was selected. The magnetic field recordings from three main magnetic observatories (marked by the red triangles in Fig. 3) starting from November 7 until the end of November 8 are obtained, which comprised 2880 data points with a sampling interval of 1 min. Magnetic derivatives against time ( $dB/dt$ ) were calculated from the magnetic field recordings that are shown in Fig. 4. It shows that the rates of magnetic field change at three observatories are almost identical. Therefore, it is reasonable and acceptable to assume the magnetic field to be uniform over the geographical area of the entire power grid. In the next calculation, the magnetic field records from BMT observatories will be used.

Based on the four-layer earth conductivity model [23] and the interpretation of existing geophysical measurements [24], [25], the ranges of the soil layer conductivities are roughly determined

TABLE I  
EFFECT OF TRUNCATION ORDER OF PC METHOD ON ERROR PERCENTAGE

$d$	Compare projects						$Q$	$L$
	Mean (%)		Standard deviation(%)		Median (%)			
	$E_x$	$E_y$	$E_x$	$E_y$	$E_x$	$E_y$		
1	5.288	0.378	23.83	14.07	10.30	2.459	5	10
2	0.261	0.012	2.627	2.382	0.476	0.016	15	30
3	0.027	0.154	2.628	3.940	0.689	0.202	35	70
4	0.061	0.013	0.390	0.767	0.071	0.129	66	132
5	0.034	0.073	0.496	1.650	0.018	0.021	126	252

Here,  $d$  is the truncation order of the PC expansions.  $Q$  is the number of polynomial terms. When we calculate the coefficients of PC expansion, we sample  $L$  (equal to  $2Q$ ) sets of samples and put them into the objective functions. So  $L$  is also the solution times to the objective function.

and their values are assumed to be of uniform distribution. Nevertheless, the uniform distribution may not be optimal, if sufficient values of soil conductivities can be acquired; then, more preferable distributions would be inferred based on Bayesian methods. Subscripts 1–4 are used to denote each layer from the top layer downwards. The thicknesses of the top three layers are 30, 60, and 60 km. The resistivity variable ranges assigned to each layer are [100, 2000], [50, 770], and [25, 2000]  $\Omega$ -m. Under a depth of 150 km, it is a bottom half-space with the resistivity from 1 to 3  $\Omega$ -m.

### B. UQ for the Maximums of Geo-Electric Fields

For geo-electric field study, the 4-D input variables are the conductivities of the four-layer earth following random distribution in their respective variable ranges. They are denoted by  $\mathbf{X} = (\xi_1, \xi_2, \xi_3, \xi_4) = (\sigma_1, \sigma_2, \sigma_3, \sigma_4)$ .

According to the distribution characteristic of input variables, 10 000 samples can be obtained and used as 10 000 input conditions. Then 10 000 outputs can be calculated either by MC method or by PC method. With these results, we can calculate the mean, standard deviation, and median of geo-electric field maximums. Taking the results of MC method as a reference, we can calculate the error percentages between the PC method and MC method. For PC method, different truncation orders have different calculation accuracies. The error percentages between two methods with different orders are compared in Table I.

It indicates that the higher the order is, the more accurate the results are. Considering that the term number and the solution time will increase along with the orders, the third order PC expansion would be appropriate. Compared with 10 000 iterations to the objective function of MC method, the third order PC method only needs to solve the objective function 70 iterations to achieve approximated accuracy.

The cumulative probability density (CDF) curves of the maximums of  $E_x$  and  $E_y$  are shown in Fig. 5, which provides the ranges of geo-electric field maximums during the storm event and the probabilities of different maximums.

### C. UQ for the Maximums of GIC

The above mentioned dc resistances of transmission lines and transformer windings are the values at specific temperatures. In

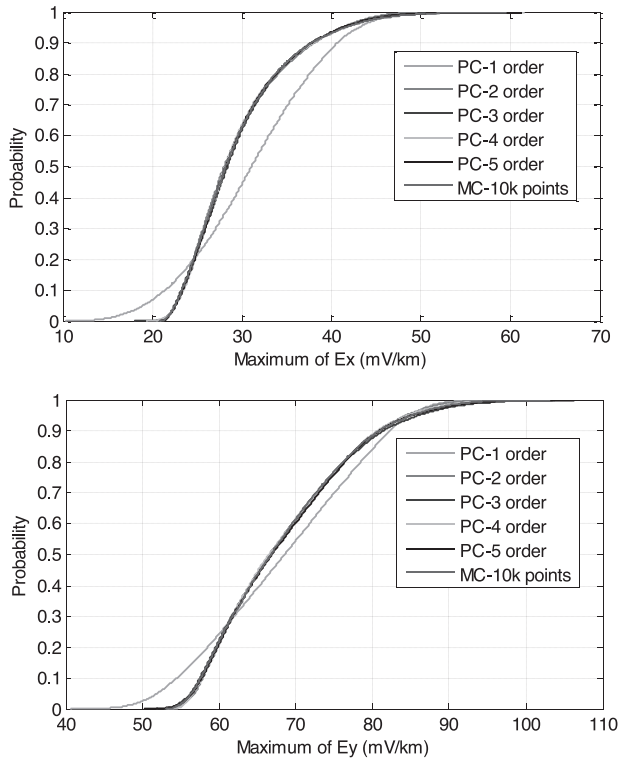


Fig. 5. Comparison of CDF of the geo-electric field maximums obtained by PC method and MC method.

273 practice, they would change with temperatures. In addition, the  
 274 product parameters of different manufacturers may be slightly  
 275 different. The grounding resistance may change with soil mois-  
 276 ture and corrosion situations of the grounding conductor. Hence,  
 277 for the UQ of GIC, dc resistances should be treated as input vari-  
 278 ables as well. The input variables are therefore 7-D, which can  
 279 be expressed by the vector of  $\mathbf{X} = (\sigma_1, \sigma_2, \sigma_3, \sigma_4, R_1, R_2, R_3)$ .  
 280 Here,  $R_1$  denotes the resistance per unit length of transmission  
 281 line,  $R_2$  denotes the winding resistance, and  $R_3$  denotes the sub-  
 282 station grounding resistance. Considering the practical operation,  
 283 we roughly assume that the transmission line resistances  
 284 vary from 0.00912 to 0.0114  $\Omega/\text{km}$ , and the values of trans-  
 285 former windings range between  $\pm 8\%$ . Considering the design  
 286 requirement of grounding resistance and the practical operation  
 287 in UHV substations, the reasonable range of grounding resis-  
 288 tance is from 0.08 to 0.12  $\Omega$ . The resistance values are assumed  
 289 to follow uniform distribution.

290 Similarly, the GIC maximums of all the substations in Sanhua  
 291 grid can be obtained by using the PC method. For example, the  
 292 CDF curves of the No.1 substation computed by the MC method  
 293 and PC method under different orders are shown in Fig. 6. It  
 294 shows that the accuracy is acceptable when the order is greater  
 295 than two. The same conclusion could be derived from other  
 296 substations.

297 The number of polynomial terms and program running time  
 298 under different orders are compared in Table II. For MC method,  
 299 it takes 3 h 26 min to finish 10 000 outputs. But even for 5-order  
 300 PC expansion including 792 polynomial terms, it would take  
 301 only about half an hour to get 10 000 outputs. Obviously, the

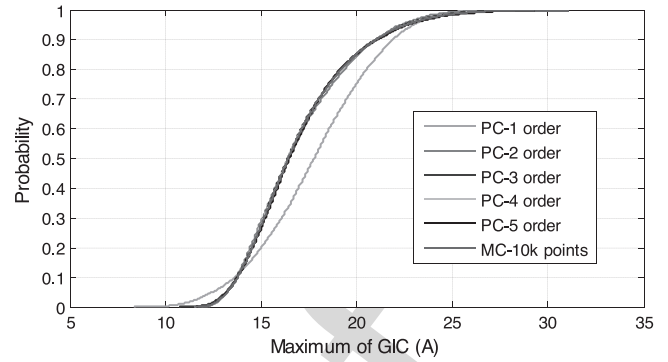


Fig. 6. Comparison of CDF curves of GIC maximums in No.1 substation calculated by PC expansions and MC method.

TABLE II  
COMPARISONS OF PC METHOD UNDER DIFFERENT ORDER

Order	1	2	3	4	5
$Q$	8	36	120	330	792
$L$	16	72	240	660	1584
$t_1$	40.068s	93.654s	4min39s	14min5s	32min24s
$t_2$	4.404s	5.630s	11.932s	34.196s	109.844s

$Q$  and  $L$  have the same meaning as those in Table I. Here,  $t_1$  is the approximate program run time to get the PC expansions, and  $t_2$  is the program run time to substitute 10 000 sample sets in the PC expansion to obtain 10 000 outputs. The main computer configuration is 8G memory and Intel i5-5200U CPU (2.2 GHz).

302 PC method can greatly shorten simulation time and increase the  
 303 computation efficiency.

304 After comprehensive comparison, we choose the 3-order PC  
 305 expansions to carry out UQ for GIC maximums. Then, we carry  
 306 out statistical analysis for the 10 000 outputs to get extra infor-  
 307 mation, such as variances, means, and cumulative probability  
 308 density. The results are shown in Fig. 7, which provides the GIC  
 309 maximums in all the 37 substations, as well as their interval  
 310 distributions. It shows that in almost half of the 37 substations,  
 311 the maximums of GIC from substation to the earth would ex-  
 312 ceed 20 A. The GIC in the Jingwest substation and the Shanghai  
 313 substation are larger than the others due to the ‘‘edge effect.’’

314 Similarly, the CDF of all output variables could be calculated.  
 315 Due to limited space, only the CDF curves and histograms of 12  
 316 crucial substations are listed in Fig. 8. The information provided  
 317 by Fig. 8 could clarify the distribution characteristics of GIC  
 318 maximums and how frequently the values may occur.

319 Obviously, for each input sample, there is a corresponding  
 320 output. And among these outputs, we can find the condition  
 321 under which the highest GIC maximums would appear. For  
 322 example, GIC time series in three substations are shown in  
 323 Fig. 9. The horizontal coordinate donates the time with the unit  
 324 of minutes. The red texts are the values of GIC maximums  
 325 during this storm event.

#### IV. SENSITIVITY STUDIES

326  
 327 The sensitivity analysis based on variance decomposition can  
 328 be used to quantify the influence of the input variables on the  
 329 output variables.

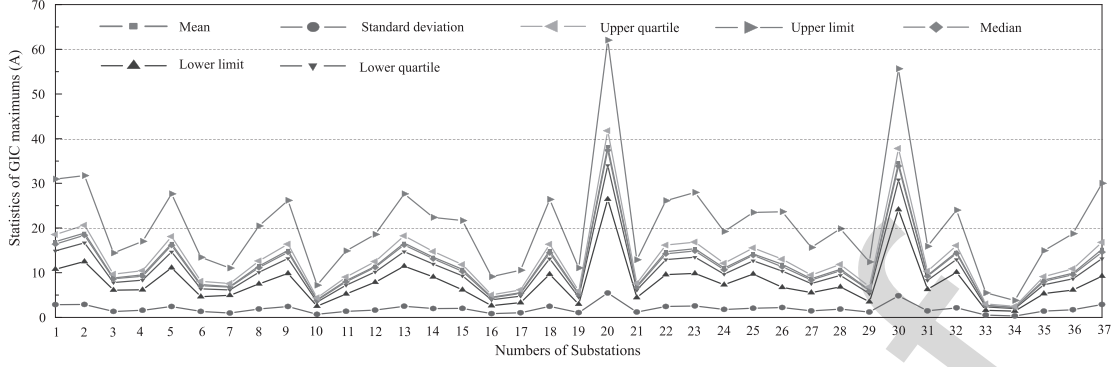


Fig. 7. Comparison of seven kinds of statistic parameters of GIC maximums in 37 substations.

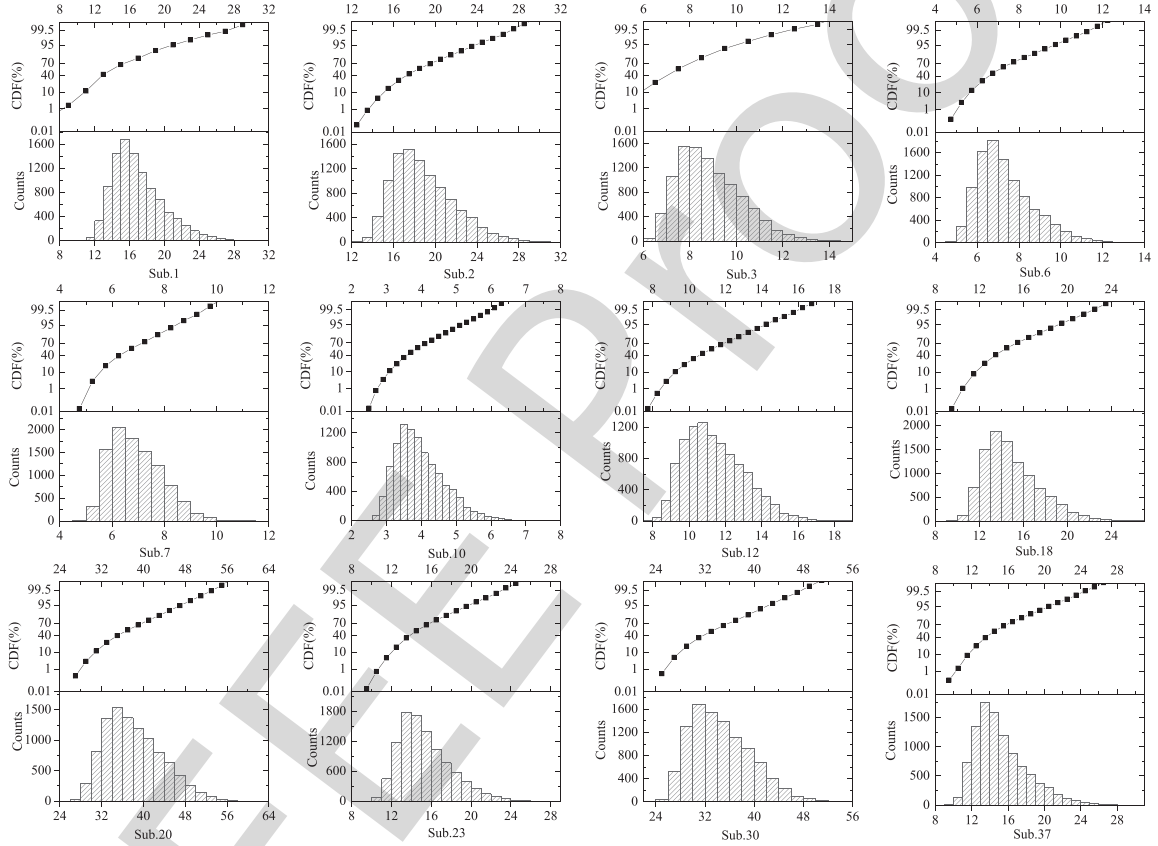


Fig. 8. Cumulative probability density curves and histograms of 12 crucial substations. The horizontal axis denotes the maximum of GIC with the unit of ampere. The numbers of substations are labeled below the graph.

330 The variance of the objective function and the partial vari-  
 331 ances of single input variable or between input variables are  
 332 denoted by  $V$  and  $V_{i_1, i_2, \dots, i_s}$ , respectively. The Sobol indices  $S_i$   
 333 and the total Sobol indices  $S_i^T$  of the response  $Y(\mathbf{X})$  with respect  
 334 to the input variables  $x_i$  are as follows [26]:

$$S_{i_1, \dots, i_s} = \frac{V_{i_1, \dots, i_s}}{V} \quad 1 \leq i_1 < \dots < i_s \leq n; \quad s = 1, 2, \dots, n$$

$$S_i^T = \sum_{\tau_i} S_{i_1, \dots, i_s}, \quad \tau_i = \{(i_1, \dots, i_s) : \exists k, 1 \leq k \leq s, i_k = i\}.$$

(14)

(15)

For  $d$ -order PC expansion, the total Sobol indices can be  
 335 estimated by  
 336

$$S_i^T = \frac{\sum \gamma_i A_{i_1, \dots, i_t}^2}{V}, \quad \gamma_i = \{(i_1, \dots, i_t) : \exists k, 1 \leq k \leq t, i_k = i\}$$

$$1 \leq i_1 < \dots < i_t \leq n; \quad t = 1, 2, \dots, d.$$

$$V = \sum_{i_1=1}^n A_{i_1}^2 + \sum_{i_1=1}^n \dots \sum_{i_d=1}^{i_{d-1}} A_{i_1, i_2, \dots, i_d}^2. \quad (16)$$

In order to illustrate the effects of all input random variables  
 337 mentioned previously on the output variables, we calculate the  
 338

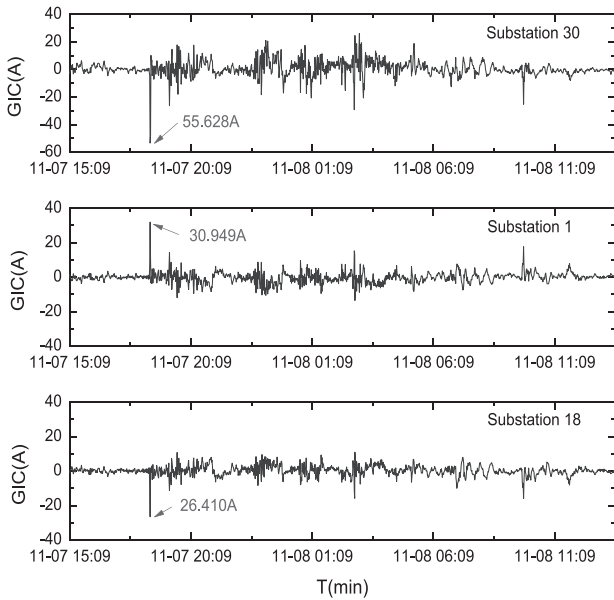


Fig. 9. Time series of GICs in three substations.

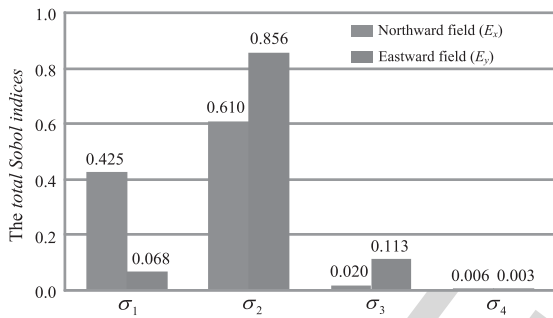


Fig. 10. Total Sobol indices of the maximums of geo-electric fields.  $\sigma_1$ ,  $\sigma_2$ ,  $\sigma_3$ , and  $\sigma_4$  are the earth conductivities of the four-layer model, respectively.

total Sobol indices with the coefficients solved above. The total Sobol indices of the maximums of geo-electric fields to the earth conductivities are presented in Fig. 10.

Regarding the example studied in this paper, it shows that the northward field is mainly related to the conductivities of the top two layers, and the eastward field is more sensitive to the conductivity of the second layer. The earth conductivity below 150 km has little effect on geo-electric fields.

The same work can be done for the GICs from substation to the ground. In Fig. 11, for the given distribution characteristics of the input variables in this paper, we list the total Sobol indices of the 12 substations considered in Section III. Obviously, the GIC maximums are more sensitive to earth conductivities than the resistances, especially to the conductivity of the second layer. The influence of the 7-D input variables on different substations is mainly due to their different geographic locations as well as their relative positions within the grid.

### V. CONCLUSION

In this paper, considering the complex and uncertain input parameters in GIC calculation, we propose an UQ model of the

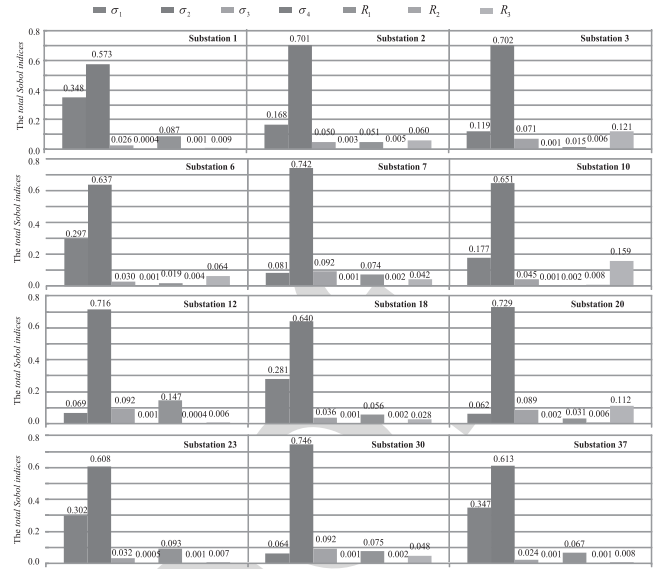


Fig. 11. Total Sobol indices of the maximums of GICs in 12 substations.

geo-electric fields and GICs. The UQ for the geo-electric fields and GICs of a UHV power grid is carried out.

The PC expansion provides an efficient surrogate model to replace the objective function which can be used to analyze the uncertainty of the origin problem easily. For the calculation of GIC under 10 000 sample sets, the computational time of the PC method takes only one fortieth of that of the MC method.

For the considered storm event, the northward fields and eastward fields vary from 18.654 to 55.791 mV/km and from 51.864 to 103.416 mV/km, respectively. In all the substations within the grid, 17 stations experience GICs exceeding 20 A in amplitude. GIC levels of some substations are relatively higher than others, especially substations No.20 and No.30.

The total Sobol indices are calculated by using the PC expansion coefficients. Sensitivity analysis shows that, the conductivity of the second layer has a greater impact on the geo-electric fields and GICs than the other layers. In different substations, the GICs are sensitive to their geological locations involving the 7-D input variables. Sufficient consideration should be given to the grounding resistance of substations when carrying out GIC evaluation and mitigation.

The proposed method can effectively offer a better understanding of the sensitivities of GICs to input uncertain variables and give a reasonable evaluation of the geomagnetic hazards to the power system. In the future, we will strive to acquire more information to set up an exact earth conductivity model for GIC UQ. Furthermore, we will monitor the substations where the GIC levels are relatively high in order to validate the computational model that makes it possible to provide predicted GIC based on the correlative predicted data of space weather.

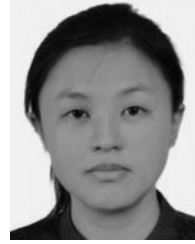
### ACKNOWLEDGMENT

The authors would like to thank the electric power design institutes for providing certain parameters of the Sanhua grid and Prof. S.-m. Wang for the useful advice on earth model.



## REFERENCES

- [1] D. H. Boteler, R. Pirjola, and H. Nevanlinna, "The effects of geomagnetic disturbances on electrical systems at the Earth's surface," *Adv. Space Res.*, vol. 22, no. 1, pp. 17–27, Sep. 1998.
- [2] R. Pirjola, "Geomagnetically induced currents during magnetic storms," *IEEE Trans. Plasma Sci.*, vol. 28, no. 6, pp. 1867–1873, Dec. 2000.
- [3] L. Bolduc, P. Langlois, and D. Boteler, "A study of geoelectromagnetic disturbances in Québec, 2. Detailed analysis of a large event," *IEEE Trans. Power Del.*, vol. 15, no. 1, pp. 272–278, Feb. 2000.
- [4] D. Boteler, R. Pirjola, A. Viljanen, and O. Amm, "Prediction of geomagnetically induced currents in power transmission system," *Adv. Space Res.*, vol. 26, no. 1, pp. 5–14, Mar. 2000.
- [5] V. V. Vakhnina, V. A. Shapovalov, V. N. Kuznetsov, and D. A. Kretov, "The influence of geomagnetic storms on thermal processes in the tank of a power transformer," *IEEE Trans. Power Del.*, vol. 30, no. 4, pp. 1702–1707, Aug. 2015.
- [6] W. A. Radasky, "Impacts of variations of geomagnetic storm disturbances on high voltage power systems," *IEEE Trans. Power Energy*, vol. 133, no. 12, pp. 931–934, Dec. 2013.
- [7] C. Barbosa, G. Hartmann, and K. Pinheiro, "Numerical modeling of geomagnetically induced currents in a Brazilian transmission line," *Adv. Space Res.*, vol. 55, no. 4, pp. 1168–1179, Nov. 2015.
- [8] Q. Liu, K. Han, and Y. Bai, "Analysis of distribution regularities and sensitivity of geomagnetically induced currents in planned Xinjiang 750 kV power grid," *Power Syst. Technol.*, vol. 41, no. 17, pp. 3678–3684, Nov. 2017.
- [9] R. Pirjola, "Review on the calculation of surface electric and magnetic fields and of GICs in ground based technological systems," *Surv. Geophys.*, vol. 23, no. 1, pp. 71–90, Jan. 2002.
- [10] D. Boteler, "The use of linear superposition in modelling geomagnetically induced currents," in *Proc. IEEE Power Energy Soc. General Meeting*, 2013, pp. 1–5.
- [11] D. H. Boteler, "The evolution of québec earth models used to model geomagnetically induced currents," *IEEE Trans. Power Del.*, vol. 30, no. 5, pp. 2171–2178, Oct. 2015.
- [12] L. Marti, C. Yiu, A. Rezaei-Zare, and D. Boteler, "Simulation of geomagnetically induced currents with piecewise layered-earth models," *IEEE Trans. Power Del.*, vol. 29, no. 4, pp. 1886–1893, Aug. 2014.
- [13] J. L. Gilbert, "Simplified techniques for treating the ocean-land interface for geomagnetically induced electric fields," *IEEE Trans. Electromagn. Compat.*, vol. 57, no. 4, pp. 688–692, Aug. 2015.
- [14] J. J. Love, G. M. Lucas, A. Kelbert, and P. A. Bedrosian, "Geoelectric hazard maps for the mid-atlantic united states: 100 year extreme values and the 1989 magnetic storm," *Geophys. Res. Lett.*, vol. 45, no. 1, pp. 5–14, Jan. 2018.
- [15] H. Karami *et al.*, "Effect of mixed propagation path on electromagnetic fields at ground surface produced by electrojet," *IEEE Trans. Electromagn. Compat.*, vol. 60, no. 6, pp. 2019–2024, Dec. 2018.
- [16] X. B. Chen, Q. T. Lu, and K. Zhang, "Review of magnetotelluric data inversion methods," *Prog. Geophys.*, vol. 26, no. 5, pp. 1607–1619, Oct. 2011.
- [17] V. D. Albertson, J. G. Kappenman, and N. Mohan, "Load-flow studies in the presence of geomagnetically-induced currents," *IEEE Trans. Power App. Syst.*, vol. PAS-100, no. 2, pp. 594–607, Feb. 1981.
- [18] R. Horton, D. Boteler, T. J. Overbye, R. Pirjola, and R. C. Dugan, "A test case for the calculation of geomagnetically induced currents," *IEEE Trans. Power Del.*, vol. 27, no. 4, pp. 2368–2373, Oct. 2012.
- [19] M. Lehtinen and R. Pirjola, "Currents produced in earthed conductor networks by geomagnetically induced electric fields," *Annales Geophysicae*, vol. 3, no. 4, pp. 479–484, Jan. 1985.
- [20] Z. Fei, Y. Huang, J. Zhou, and Q. Xu, "Uncertainty quantification of crosstalk using stochastic reduced order models," *IEEE Trans. Electromagn. Compat.*, vol. 59, no. 1, pp. 228–239, Feb. 2017.
- [21] S. Oladyskhin and W. Nowak, "Data-driven uncertainty quantification using the arbitrary polynomial chaos expansion," *Rel. Eng. Syst. Safety*, vol. 106, no. 4, pp. 179–190, May 2012.
- [22] D. Xiu and G. E. Karniadakis, "The Wiener–Askey polynomial chaos for stochastic differential equations," *SIAM J. Sci. Comput.*, vol. 24, no. 2, pp. 619–644, Oct. 2002.
- [23] K. Zheng, "Research on influence factors and modelling methods of geomagnetically induced currents in large power grid," *Ph.D. dissertation*, North China Elect. Power Univ., Beijing, China, 2014.
- [24] W. Wei *et al.*, "Geoelectric structure of lithosphere beneath eastern North China: Features of a thinned lithosphere from magnetotelluric soundings," *Earth Sci. Frontiers*, vol. 15, no. 4, pp. 204–216, Jul. 2008.
- [25] Y. Liu and Y. Xu, "Lithospheric electrical characteristic in South China and its geodynamic implication," *Chin. J. Geophys.*, vol. 56, no. 12, pp. 204–216, Dec. 2013.
- [26] I. M. Sobol, "Global sensitivity indices for nonlinear mathematical models and their Monte Carlo estimates," *Math. Comput. Simul.*, vol. 55, no. 1/3, pp. 271–280, Feb. 2001.



**Qing Liu** was born in 1978. She received the B.Sc. and M.S. degrees in electrical engineering from Chongqing University, Chongqing, China, in 2000, and Xi'an Jiaotong University, Xi'an, China, in 2005, respectively. She is currently working toward the Ph.D. degree in electrical engineering at Xi'an Jiaotong University.

She is also an Associate Professor with the Xi'an University of Science and Technology, Xi'an, China. Her research interest includes modeling and assessing geomagnetically induced currents in power grids.



**Yan-zhao Xie (M'12)** was born in 1973. He received the Ph.D. degree in electrical engineering from Tsinghua University, Beijing, China, in 2005.

Since 2016, he is the Director of the National Center for International Research on Transient Electromagnetics and Applications. He is currently a Professor with Xi'an Jiaotong University, Xi'an, China. His research interests include electromagnetic transients in power system, electromagnetic compatibility, etc.



**Ning Dong** received the B.Sc. degree in electrical engineering from Xi'an Jiaotong University, Xi'an, China, in 2016. She is currently working toward the Ph.D. degree at Xi'an Jiaotong University.

Her research interest includes modeling and UC of multiconductor transmission lines coupling.



**Yu-hao Chen** received the B.Sc. degree in electrical engineering from Xi'an Jiaotong University, Xi'an, China, in 2015, where he is currently working toward the Ph.D. degree in electrical engineering.

His research interest is the effect evaluation of electromagnetic environments.



**Min-zhou Liu** received the B.Sc. degree in electrical engineering from Xi'an Jiaotong University, Xi'an, China, in 2017, where he is currently working toward the M.S. degree.

His research interests include the effect evaluation of electromagnetic environments and reliability evaluation of power system.



**Quan Li** is a Tenure Lecturer with the University of Edinburgh, Edinburgh, U.K., and Theme Leader of Applied Superconductivity.

His research interests include electromagnetism and superconducting applications in energy and healthcare sectors.

Dr. Li is a Fellow of the Higher Education Academy.